Applied Physics Letters

800 meV localization energy in GaSb/GaAs/$Al_{0.3}Ga_{0.7}As$ quantum dots

Cite as: Appl. Phys. Lett. **102**, 052115 (2013); https://doi.org/10.1063/1.4791678
Submitted: 20 December 2012 • Accepted: 29 January 2013 • Published Online: 07 February 2013

T. Nowozin, L. Bonato, A. Högner, et al.

800 meV localization energy in GaSb/GaAs/$Al_{0.3}Ga_{0.7}As$ quantum dots

T. Nowozin,[1,a)] L. Bonato,[1] A. Högner,[1] A. Wiengarten,[1] D. Bimberg,[1,b)] Wei-Hsun Lin,[2] Shih-Yen Lin,[2] C. J. Reyner,[3] Baolai L. Liang,[3] and D. L. Huffaker[3]
[1]*Institut für Festkörperphysik, Technische Universität Berlin, Hardenbergstrasse 36, 10623 Berlin, Germany*
[2]*Research Center for Applied Sciences, Academia Sinica, Taipei, Taiwan*
[3]*Department of Electrical Engineering and California Nano-Systems Institute, University of California at Los Angeles, Los Angeles, California 90095, USA*

(Received 20 December 2012; accepted 29 January 2013; published online 7 February 2013)

The localization energies, capture cross sections, and storage times of holes in GaSb quantum dots (QDs) are measured for three GaSb/GaAs QD ensembles with different QD sizes. The structural properties, such as height and diameter, are determined by atomic force microscopy, while the electronic properties are measured using deep-level transient spectroscopy. The various QDs exhibit varying hole localization energies corresponding to their size. The maximum localization energy of 800 (±50) meV is achieved by using additional $Al_{0.3}Ga_{0.7}As$ barriers. Based on an extrapolation, alternative material systems are proposed to further increase the localization energy and carrier storage time of QDs. © *2013 American Institute of Physics*. [http://dx.doi.org/10.1063/1.4791678]

As a result of their type-II properties, the band gap difference between Sb-based III-V materials and the surrounding matrix material (i.e., GaAs or $Al_xGa_{1-x}As$) leads to a giant valence band offset. Especially, in comparison with the well-known InAs/GaAs material system, quantum dots (QDs) based on GaSb/GaAs can offer confining potentials for holes, which are twice to three times as large. This makes GaSb/GaAs a particularly interesting heterostructure for charge storage applications in which holes are used as information carriers. Concepts for QD-based memories were previously demonstrated.[1–5]

GaSb/GaAs QDs have been grown by molecular beam epitaxy (MBE)[6,7] and metal-organic chemical vapor deposition (MOCVD),[8,9] their structure has been analyzed by cross-sectional scanning tunneling microscopy (X-STM),[10–12] their optical properties were studied,[6,13] as well as their electronic properties.[12,14,15] Nevertheless, consistent data on localization energies and capture cross sections for holes, which are crucial parameters for any process involving hole dynamics and the ability of the QDs to confine and store holes, are missing.

In this letter, we report on the electronic properties of a set of three GaSb/GaAs QD samples, in which the QDs have varying lateral extension and height. The size of the QDs is studied by atomic force microscopy (AFM) on uncapped QD samples. The electronic properties of the QDs are studied by charge-selective deep-level transient spectroscopy (DLTS),[15–17] which allows to determine the localization energy and the apparent capture cross section of the QD ensemble as key electronic properties. The theoretical dependence of the storage time on the localization energy and the apparent capture cross section are used to give an extrapolation for the storage time at room temperature, based on which alternative III–V material systems are proposed to achieve non-volatility (>10 yr) in a QD-based memory.

In the voltage regime where the measurements are performed, tunneling emission can be neglected,[18] and the trapped holes inside the QDs are emitted by thermal activation only. The thermal emission rate of holes from the QDs is[16]

$$e_a = \gamma T^2 \sigma_\infty exp(-E_a/kT), \quad (1)$$

where E_a is the activation energy, T the temperature, k the Boltzmann constant, σ_∞ is the apparent capture cross section for $T = \infty$, and γ is a temperature-independent constant. The emission rate depends on the energetic barrier (activation energy) E_a, which the holes have to overcome during the thermal emission process, and the apparent capture cross section σ_∞, which is a measure of the ability of the QDs to scatter free holes from the surrounding matrix into its potential well. It is an expression of how well the QDs couple to the surrounding material in order to dissipate the energy and momentum of the scattered holes, i.e., by Auger scattering or multi-phonon emission.[19] As re-capture of holes also occurs during the thermal emission process, the capture cross section also determines the emission rate (retention time) of the holes in the QDs.[19,20] According to Eq. (1), the thermal emission rate is directly proportional to σ_∞. To get a rule of thumb for the effect of the activation energy E_a on the emission rate, we use the laws for logarithm conversion and get an effect on the emission rate (retention time) of one order of magnitude for every 2.3 × kT. At 300 K, this would mean that the storage time would increase by one order of magnitude for each additional 60 meV of activation energy.

Three different samples were studied in this work. They all contain a layer of self-assembled GaSb/GaAs QDs embedded into a pn-diode structure, which is schematically shown in the inset of Fig. 2(a) and described in Ref. 15.

Samples A and C were grown at Academia Sinica, Taiwan. The QDs in both samples have nominally the same growth conditions for the QD layer, of which details can be found in Refs. 21 and 22. The GaSb QD structures of the two samples are both grown at 470 °C. The pre- and post- Sb soaking time were 15 s and 120 s, respectively. During the post-soaking procedure, the Sb flux is kept at 1.5×10^{-7} Torr (beam equivalent flux pressure, BEP).

a)Electronic mail: nowozin@sol.physik.tu-berlin.de.
b)Also at King Abdulaziz University, Jeddah, Saudi Arabia.

In addition to the QD layer, sample C contains two $Al_{0.3}Ga_{0.7}As$ barriers, in between which the QD layer is sandwiched. The barriers increase the emission barrier by an additional valence band offset of $\Delta_{VB} = 162$ meV (based on an 34:66 split of the band gap difference between GaAs and $Al_{0.3}Ga_{0.7}As$ (Ref. 23)).

Sample B was grown at UCLA in a solid-source MBE reactor using cracked arsenic and antimony sources. After GaAs oxide desorption at 610 °C, an undoped GaAs buffer is grown at 580 °C prior to the diode structure. The growth rate is approximately 1 μm/h and the V/III ratio is approximately 15. The quantum dot growth proceeds by lowering the substrate temperature to 480 °C and the growth rate to 0.15 μm/h. The V/III ratio for the GaSb quantum dots is 1.05. After closing the As_2 beam and soaking the substrate with Sb_2, 3.5 ML of GaSb are deposited and the RHEED pattern changes from streaks (2D growth) to spotty (3D island growth). A 10-nm-thick cap of GaAs is deposited at the QD growth temperature, before heating the substrate back to 580 °C and completing the rest of the diode structure. The dopants used are silicon (n-type) and beryllium (p-type).

Uncapped GaSb/GaAs QDs with identical growth parameters as for the QDs in samples A, B, and C were grown with each individual growth batch and analyzed by AFM measurements. The AFM pictures are shown in Fig. 1. The QDs have a dome-like shape and their mean diameter varies from 20 (±4) nm for sample A, 24 (±4) nm for sample C, up to a diameter of 40 (±4) nm for sample B. The mean heights vary between 2 nm for sample A, 2.5 nm for sample C, and 4.5 nm for sample B. The area densities are 5×10^{10} cm^{-2} for sample A, 4×10^{10} cm^{-2} for sample B, and 3×10^{10} cm^{-2} for sample C. Although grown with nominally the same growth parameters, the QDs of samples A and C have different sizes. We attribute this to the run-to-run variation of the chamber, since the samples were grown 1.5 yr apart from each other.

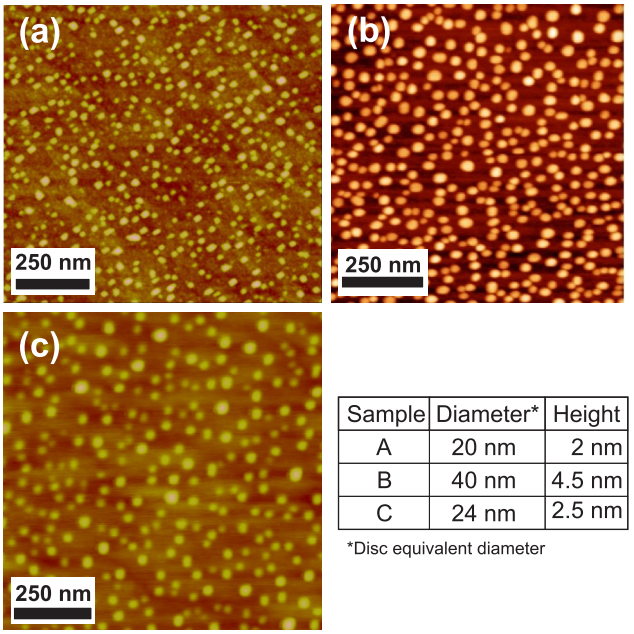

Sample	Diameter*	Height
A	20 nm	2 nm
B	40 nm	4.5 nm
C	24 nm	2.5 nm

*Disc equivalent diameter

FIG. 1. AFM measurements of uncapped GaSb/GaAs QD ensembles corresponding to growth parameters identical to samples (a) A, (b) B, and (c) C. The sizes are given in the table.

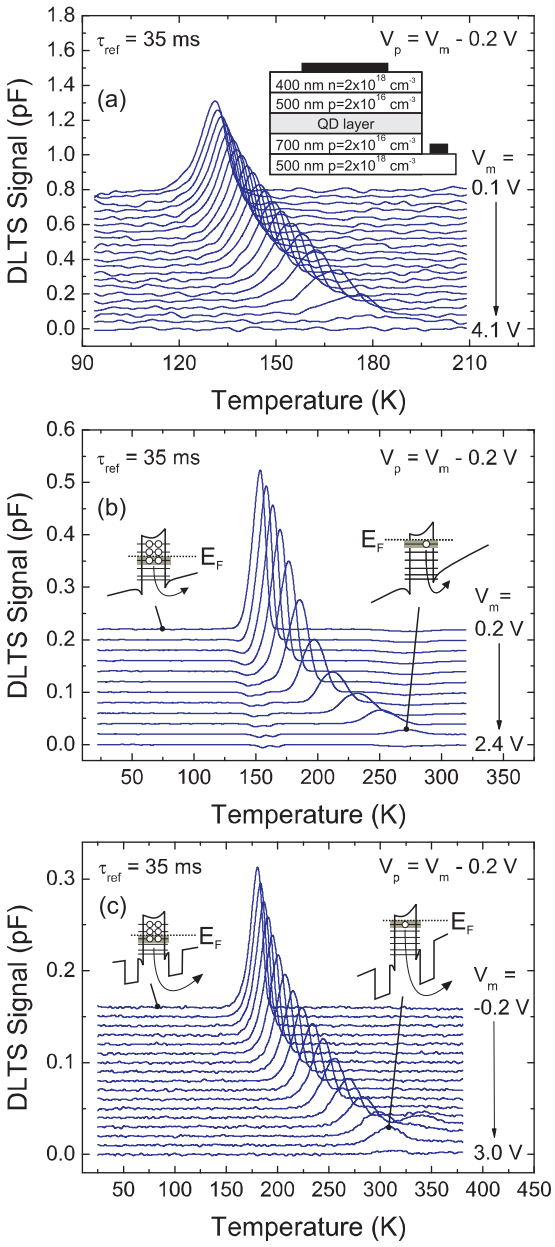

FIG. 2. Charge-selective DLTS measurements with a reference time constant of $\tau_{ref} = 35$ ms and different measurement voltages V_m. (a) Sample A: GaSb/GaAs QDs in GaAs pn-diode. (b) Sample B: GaSb/GaAs QDs in GaAs pn-diode. (c) Sample C: GaSb/GaAs QDs with two additional $Al_{0.3}Ga_{0.7}As$ barriers.

The samples are processed into round mesa-structures by standard optical lithography and chemical wet-etching techniques. The contact layers are metallized by Ni/AuGe/Au (n-side) and Ti/Pt/Au (p-side) and subsequent annealing for 3 min at 400 °C to form Ohmic contacts.

The samples are analyzed by charge-selective DLTS,[15,16,24] which allows a detailed study of the electronic properties of the QD ensemble. The bias voltage range in which charging and discharging of the QDs occur is determined by capacitance-voltage (C-V) measurements and the values are used in the following charge-selective DLTS experiments.[15] The charging pulse voltage is selected in such a way that only very few holes are captured and emitted from the QDs (ideally one hole per QD). The capacitance transients are measured with a frequency of 1 MHz and averaged several times.

Sample A: The measurement bias is set from $V_m = 0.1$ to $V_m = 4.1$ in steps of 0.2 V while setting the pulse bias to $V_p = V_m - 0.2$V. The temperature is swept from 92 K to 210 K. *Sample B*: $V_m = 0.2$ to $V_m = 2.4$ in steps of 0.2 V, pulse bias set to $V_p = V_m - 0.2$V. The temperature is swept from 25 K to 320 K. *Sample C*: $V_m = -0.2$ to $V_m = 3.0$ in steps of 0.2 V, pulse bias set to $V_p = V_m - 0.2$V. The temperature is swept from 25 K to 380 K.

The charge-selective DLTS graphs for the three samples are shown in Fig. 2 for a reference time constant $\tau_{ref} = 35$ ms. Clear features can be seen in all three graphs due to the hole emission from the QD ensemble. When the measurement bias is increased (reverse direction), the peak shifts to higher temperatures, which indicates that deeper hole states in the QDs are successively probed at each V_m. The DLTS graphs are analyzed by extracting the peak positions for a set of different reference time constants and plotting the data as an Arrhenius plot (not shown). Using Eq. (1), the data points are fitted, and from the slope the activation energy E_a, and from the intercept the apparent capture cross section σ_∞ are derived for each DLTS graph.[25]

The activation energies E_a and apparent capture cross sections σ_∞ for the three samples are depicted in Fig. 3. For sample A, an increase of the activation energy from 300 meV up to 460 meV can be observed when the measurement bias is increased. The apparent capture cross section stays roughly constant around 10^{-12} cm^2 and increases only for the highest reverse bias at $V_m = 3.8$ V. As the signal completely vanishes for a reverse bias larger than 3.8 V, the value is equal to the activation energy of the ground state. Hence, the localization energy is $E_{loc} = 460\,(\pm 20)$ meV with $\sigma_\infty = 7 \times 10^{-12}$ cm^2.

The activation energies in sample B increase from 340 meV at $V_m = 0.2$ V to 760 meV at $V_m = 2.2$ V, while the apparent capture cross section increases from 10^{-13} cm^2 to about 10^{-10} cm^2. Hence, we get $E_{loc} = 760(\pm 20)$ meV with $\sigma_\infty = 5 \times 10^{-11}$ cm^2.

For sample C, the activation energy increases from 420 meV at $V_m = -0.2$ V (forward direction) to 800 meV at $V_m = 2.8$ V, while the apparent capture cross section roughly stays constant around 10^{-12} cm^2. The localization energy of the GaSb-QDs with the $Al_{0.3}Ga_{0.7}As$ barriers is then $E_{loc} = 800(\pm 50)$ meV with $\sigma_\infty = 5 \times 10^{-12}$ cm^2. To get the localization energy of the GaSb QDs only, the height of the $Al_{0.3}Ga_{0.7}As$ barriers has to be subtracted. When assuming a 66:34 split of the band offsets between GaAs and $Al_{0.3}Ga_{0.7}As$, the valence band offset amounts to $\Delta E_{VB} = 164$ meV.[23] Within the error margin, we then get $E_{loc} = 640(\pm 50)$ meV with $\sigma_\infty = 5 \times 10^{-12}$ cm^2 for the GaSb QDs only.

We attribute the increase of localization energy of the different samples (in the sequence A, C, B; QD localization energy only) to an increase of the size of the QDs in the ensembles, which quantum mechanically lowers the ground state in the potential well of the QD and increases the emission barrier.

From the localization energies E_{loc} and the apparent capture cross sections σ_∞, the storage times at 300 K can be derived as the inverse of the emission rate in Eq. (1). The values previously determined in other works[12,24,26,27] and in this work, together with the theoretical storage times for different capture cross sections, are shown in Fig. 4. Compared to the other QDs, the QD ensembles studied in this work all have a large apparent capture cross section. Hence, the storage time is lower than for QDs with the same localization energies. As the apparent capture cross sections vary by about 5 orders of magnitude, the extrapolation to storage times of 10 yr at 300 K (required for non-volatility) can only give a range of minimum localization energies which have to be achieved. The required localization energy ranges from 1.15 eV for $\sigma_\infty = 10^{-15}$ cm^2 to 1.45 eV for $\sigma_\infty = 10^{-10}$ cm^2. Two material systems able to provide such large localization energies are given in the graph. GaSb/$Al_{0.9}Ga_{0.1}As$ QDs can reach $E_{loc} = 1.25$ eV, while GaSb/GaP QDs can reach ~1.2–1.4 eV.[23,28] Using $Al_xGa_{1-x}P$ instead of GaP would further increase the localization energy by another 500 meV. In principle, large localization energies (~2 eV) should also be achievable for electrons in nitride-based QD systems.[29] The capture cross section could also be altered in order to increase the storage time. It depends on the hole wave functions in the QDs, the coupling to the phonon bath, and possible Auger scattering. However, a precise modeling of all three effects, let alone

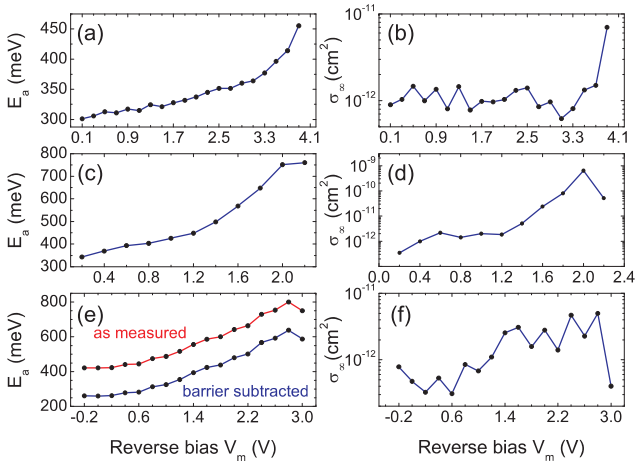

FIG. 3. Activation energies E_a and apparent capture cross sections σ_∞ for holes for each individual measurement bias V_m. (a) and (b) Sample A. (c) and (d) Sample B. (d) and (f) Sample C.

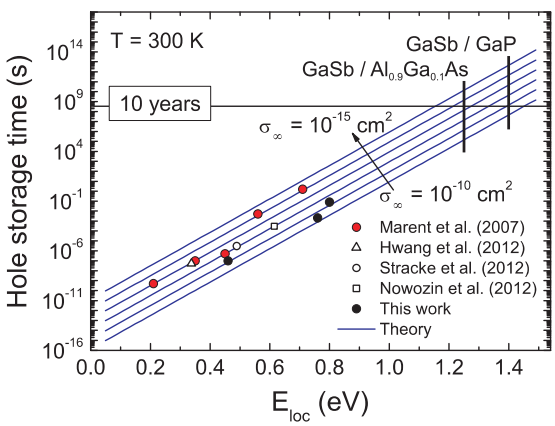

FIG. 4. Hole storage time in quantum dots as a function of the localization energy E_{loc} for different values of the apparent hole capture cross section σ_∞. 10 yr of storage time is required for non-volatility. The other values can be found in Refs. 12, 24, 26, and 27.

their precise control during epitaxial growth, has yet to be achieved.

In summary, we have studied the structural properties of GaSb/GaAs quantum dots with AFM, while the localization energies and the apparent capture cross sections were determined by DLTS. Each sample studied exhibits QD ensembles of different mean sizes, ranging from 20 nm to 40 nm in width, and 2 nm to 4.5 nm in height. The hole localization energies of the QDs are found to increase by the same order as the sizes from 460 (±20) meV to 760 (±20) meV with apparent capture cross sections around $\sigma_\infty = 10^{-12}\,\mathrm{cm}^2$. A maximum localization energy of 800 (±50) meV was found for GaSb QDs with additional $Al_{0.3}Ga_{0.7}As$ barriers—the highest value ever measured for self-assembled QDs. In order to further increase the localization energy, and hence the hole storage time in QDs, increasing the Al content in $GaSb/Al_xGa_{1-x}As$ QDs, the use of GaP as matrix material and nitride-based heterostructures are proposed.

The authors acknowledge the support by the EC NanoSci-E+ Project QD2D (BI284/30-1), DFG Contract No. BI284/29-1, BMBF Project HOFUS, the DAAD PPP Taiwan program, and Project NSC 101-2628-E-001-001. C.J.R. acknowledges support from the US DoD Science, Mathematics and Research for Transformation Scholarship.

[1]C. Balocco, A. M. Song, and M. Missous, Appl. Phys. Lett. **85**, 5911 (2004).
[2]D. Nataraj, N. Ooike, J. Motohisa, and T. Fukui, Appl. Phys. Lett. **87**, 193103 (2005).
[3]M. Geller, A. Marent, T. Nowozin, D. Bimberg, N. Akçay, and N. Öncan, Appl. Phys. Lett. **92**, 092108 (2008).
[4]A. Marent, T. Nowozin, J. Gelze, F. Luckert, and D. Bimberg, Appl. Phys. Lett. **95**, 242114 (2009).
[5]A. Marent, T. Nowozin, M. Geller, and D. Bimberg, Semicond. Sci. Technol. **26**, 014026 (2011).
[6]F. Hatami, N. N. Ledentsov, M. Grundmann, J. Böhrer, F. Heinrichsdorff, M. Beer, D. Bimberg, S. S. Ruvimov, P. Werner, U. Gösele, J. Heydenreich, U. Richter, S. V. Ivanov, B. Y. Meltser, P. S. Kop'ev, and Z. I. Alferov, Appl. Phys. Lett. **67**, 656 (1995).
[7]C.-K. Sun, G. Wang, J. E. Bowers, B. Brar, H.-R. Blank, H. Kroemer, and M. H. Pilkuhn, Appl. Phys. Lett. **68**, 1543 (1996).
[8]B. M. Kinder and E. M. Goldys, Appl. Phys. Lett. **73**, 1233 (1998).
[9]L. Müller-Kirsch, R. Heitz, U. W. Pohl, D. Bimberg, I. Häusler, H. Kirmse, and W. Neumann, Appl. Phys. Lett. **79**, 1027 (2001).
[10]R. Timm, H. Eisele, A. Lenz, S. K. Becker, J. Grabowski, T. Y. Kim, L. Müller-Kirsch, K. Pötschke, U. W. Pohl, D. Bimberg, and M. Dähne, Appl. Phys. Lett. **85**, 5890 (2004).
[11]E. P. Smakman, J. K. Garleff, R. J. Young, M. Hayne, P. Rambabu, and P. Koenraad, Appl. Phys. Lett. **100**, 142116 (2012).
[12]T. Nowozin, A. Marent, L. Bonato, A. Schliwa, D. Bimberg, E. P. Smakman, J. K. Garleff, P. M. Koenraad, R. J. Young, and M. Hayne, Phys. Rev. B **86**, 035305 (2012).
[13]E. R. Glaser, B. R. Bennet, B. V. Shannabrook, and R. Magno, Appl. Phys. Lett. **68**, 3614 (1996).
[14]R. Magno, B. R. Bennett, and E. R. Glaser, J. Appl. Phys. **88**, 5843 (2000).
[15]M. Geller, C. Kapteyn, L. Müller-Kirsch, R. Heitz, and D. Bimberg, Appl. Phys. Lett. **82**, 2706 (2003).
[16]D. V. Lang, J. Appl. Phys. **45**, 3023 (1974).
[17]C. M. A. Kapteyn, M. Lion, R. Heitz, D. Bimberg, P. N. Brunkov, B. V. Volovik, S. G. Konnikov, A. R. Kovsh, and V. M. Ustinov, Appl. Phys. Lett. **76**, 1573 (2000).
[18]T. Nowozin, A. Marent, M. Geller, D. Bimberg, N. Akçay, and N. Öncan, Appl. Phys. Lett. **94**, 042108 (2009).
[19]J. Bourgoin and M. Lannoo, *Point Defects in Semiconductors II—Experimental Aspects*, Springer Series in Solid-State Sciences Vol. 35 (Springer, Berlin, 1983).
[20]P. Blood and J. W. Orton, *The Electrical Characterization of Semiconductors: Majority Carriers and Electron States* (Academic, London, 1992).
[21]S.-Y. Lin, C.-C. Tseng, W.-H. Lin, S.-C. Mai, S.-Y. Wu, S.-H. Chen, and J.-I. Chyi, Appl. Phys. Lett. **96**, 123503 (2010).
[22]C.-C. Tseng, S.-C. Mai, W.-H. Lin, S.-Y. Wu, B.-Y. Yu, S.-H. Chen, S.-Y. Lin, J.-J. Shyue, and M.-C. Wu, IEEE J. Quantum Electron.**47**, 335 (2011).
[23]I. Vurgaftman, J. R. Meyer, and L. R. Ram-Mohan, J. Appl. Phys. **89**, 5815 (2001).
[24]A. Marent, M. Geller, A. Schliwa, D. Feise, K. Pötschke, D. Bimberg, N. Akçay, and N. Öncan, Appl. Phys. Lett. **91**, 242109 (2007).
[25]Assuming an effective hole mass of $m^* = 0.5$.
[26]J. Hwang, A. J. Martin, J. M. Millunchick, and J. D. Phillips, J. Appl. Phys. **111**, 074514 (2012).
[27]G. Stracke, A. Glacki, T. Nowozin, L. Bonato, S. Rodt, C. Prohl, A. Lenz, H. Eisele, A. Strittmatter, A. Schliwa, U. W. Pohl, and D. Bimberg, Appl. Phys. Lett. **101**, 223110 (2012).
[28]D. Bimberg, A. Marent, T. Nowozin, and A. Schliwa, Proc. SPIE **7947**, 79470L (2011).
[29]A. D. Andreev and E. P. OReilly, Phys. Rev. B **62**, 15851 (2000).